DOI 10.1007/s12182-014-0365-y

Paleoporosity and critical porosity in the accumulation period and their impacts on hydrocarbon accumulation—A case study of the middle Es_3 member of the Paleogene formation in the Niuzhuang Sag, Dongying Depression, Southeastern Bohai Bay Basin, East China

Liu Mingjie[1]*, Liu Zhen[2], Sun Xiaoming[2] and Wang Biao[3]

[1] School of Geoscience and Technology, Southwest Petroleum University, Chengdu, Sichuan 610500, China
[2] State Key Laboratory of Petroleum Resources and Prospecting, China University of Petroleum (Beijing), Beijing 102249, China
[3] Research Institute of Geophysical Exploration of Huabei Oilfield, CNPC, Cangzhou, Hebei 062550, China

Abstract: Similar reservoir sandbodies and fault conduit systems in the sandstone reservoirs in the middle Es_3 member of the Niuzhuang Sag have been problematic for a long time. The following problems remain unsolved: 1) The distribution of sandstone porosity is inconsistent with the hydrocarbon accumulation. The oil sandstones have low porosity instead of high porosity. 2) Sandstones, which have the same properties, have different levels of oiliness, and the sandstones with almost the same properties show different degrees of oil-bearing capacity. This study analyzes the condition of reservoirs in the research area during the accumulation period in terms of paleoporosity estimation and discusses the critical porosity of the sandstone reservoirs during the same period. The following conclusions can be drawn from the results. 1) Although reservoir properties are low at present and some reservoirs have become tight, the paleoporosity ranging from 18% to 25% is greater than the critical porosity of 13.9%. As the loss of porosity is different in terms of burial history, the present porosity cannot reflect porosity during the accumulation period. Similarly, high porosity during the accumulation period does not indicate that the present porosity is high. 2) The present reservoir location is consistent with the distribution of high paleoporosity during the accumulation period. This result indicates that high porosity belts are prone to hydrocarbon accumulation because of the dominant migration pathways generated as a result of property discrepancies under similar fault conduit conditions. Consequently, the hydrocarbon mainly accumulates in high porosity belts. Paleoporosity during the accumulation period is found to be a vital controlling factor. Therefore, high paleoporosity sandstones in the middle Es_3 member of the Niuzhuang Sag have great potential for future exploration.

Key words: Paleoporosity, critical porosity, dominant migration pathways, hydrocarbon accumulation, middle Es_3 member, Niuzhuang Sag, Bohai Bay Basin

1 Introduction

Hydrocarbon mainly migrates during the accumulation period. Both primary and secondary migration is closely related to the properties of reservoirs. The capacity of the hydrocarbon to migrate to sandstone reservoirs depends on the pressure difference between the source rocks and the reservoir rocks and indicates the lower limit of sandstone reservoirs in the accumulation period. The indicated lower limit is a critical property of sandstone (Liu et al, 2006; 2007a; 2012). Hydrocarbon can accumulate only if reservoir porosity is greater than the critical porosity.

Several studies focus on the lower limit of the petroliferous reservoir, and many methods have been proposed to determine the cutoff value (Guo, 2004; Wang et al, 2009; Cao et al, 2009). In addition, quantitative analyses have been performed on the lower porosity limit (Pang et al,

*Corresponding author. email: liumingjieldd@163.com
Received September 28, 2013

2003; Zhu et al, 2006; Zhu, 2008; Jiao et al, 2009).

Although much research has been done on the cutoff value of sandstone, these studies focus only on the accumulative condition of the reservoir at present. The critical porosity of the reservoir during the accumulation period is seldom studied. By researching the main controlling factors of lithologic reservoirs in different types of basins, Liu et al (2006; 2007a; 2012) proposed the theory of four-factors mainly controlling accumulation, wherein the critical porosity during the accumulation period was determined to be one of the factors. Pan et al (2011a) determined that the critical porosity of tight sandstone in the Chang 8 member in the Zhenjing area of the Ordos Basin was 10.5%; in the Xifeng area, the critical porosity of the Chang 8 member sandstone was determined to be 10.8% (Guo et al, 2012b; Chen et al, 2012).

Several problems have remained unsolved for a long time in the middle Es_3 member of the Niuzhuang Sag. The oiliness of sandstones in the same reservoir is different, thus indicating that the sandstones with low properties possess superior oil-bearing capacity; the oil-bearing sandstones with similar properties have different degrees of oil-bearing capacity. Conventional accumulation theories have been unable to provide satisfactory solutions to these problems, as the present properties will not be the same as the properties during the accumulation period. In this study, we attempt to examine this by analyzing the relation between reservoir porosity and hydrocarbon formation and enrichment.

2 Geologic setting and stratigraphy

The Bohai Bay Basin, an important hydrocarbon-producing basin in China, is located in eastern China and covers an area of approximately 200,000 km^2. Since the Paleogene period, this basin has undergone complex tectonic evolution, which can be divided into the synrift stage and the postrift stage (Hu et al, 2001; Qi et al, 2008; Li et al, 2010; Li et al, 2013). The Bohai Bay Basin consists of several sub-basins, namely, the Liaohe, Liaodong Bay, Bozhong, Jiyang, Huanghua, Jizhong, and Linqing, as shown in Fig. 1(a) (Gong, 1997).

The Dongying Depression lies south of the Jiyang Sub basin with an area of 5,850 km^2 (Zhang et al, 2009). It is further subdivided into four sags (the Minfeng Sag, the Lijin Sag, the Niuzhuang Sag, and the Boxing Sag) by several normal faults and an uplift in the central anticline belt (Fig. 1(b)). The Dongying Depression is an asymmetric half graben lacustrine basin that developed as a result of a Tertiary rift. As shown in Fig. 1(c), the depression has five secondary tectonic zones from north to south; the northern steep slope zone, the northern zone (Lijin Sag), the central anticline zone, the southern zone (Niuzhuang Sag), and the southern gentle slope zone (Chen et al, 2008; Guo et al, 2010).

The depression is filled with Cenozoic sediments, which are formations from the Paleogene, Neogene, and Quaternary periods. As shown in Fig. 2, the formations from the Paleogene period are the Kongdian (Ek), Shahejie (Es), and Dongying (Ed); the formations from the Neogene period are the Guantao (Ng) and Minghuazhen (Nm); and the formation from the Quaternary period is the Pingyuan (Qp). Detailed descriptions of the Paleogene stratigraphy have been provided by several authors (Zhang et al, 2004; Zhang et al, 2010; Guo et al, 2012a). The most important petroleum generation and accumulation layer of Es can be divided into four members: Es_1 to Es_4 in descending order. The Es_3 has a thickness ranging from 700 m to 1,200 m and is characterized by lacustrine oil shale with high sedimentation rates, dark gray mudstones, and calcareous mudstones. Es_3 can be further divided into three, namely, the upper Es_3, the middle Es_3, and the lower Es_3 members (Lampe et al, 2012).

The Niuzhuang Sag, which is located southeast of the Dongying Depression, covers an area of 600 km^2 that extends from east to west. This sag has simple tectonic features that are composed primarily of synclines. Few faults exist in this area, except at the boundaries of the rift basin. In the Niuzhuang Sag, the strata generally develop completely. This study mainly focuses on the western part of the Niuzhuang Sag and the middle Es_3 member. When the target stratum was deposited, tectonic movement was strong, and the basin subsided rapidly. Therefore, large amounts of detrital materials were transported into the basin and formed delta and turbidite fan sedimentary facies (Li, 2004; Chen et al, 2009).

3 Method

3.1 The principle of paleoporosity estimation

The key point of this research is estimating the paleoporosity during the accumulation period. In this study, we apply the principle of effect-oriented simulation to estimate paleoporosity in the accumulation period. According to the porosity variation effect, the process of porosity evolution can be divided into the increasing porosity and the decreasing porosity models (Fig. 3). When the two models are superimposed at the same time or at the same burial depth, the actual porosity in geological history is obtained.

3.2 Decreasing porosity model

The decreasing porosity of the middle Es_3 member has been affected by compaction and cementation, and the effect of decreasing porosity continues with the burial of strata. In this process, compaction plays a major role, particularly in the shallow layers. However, both compaction and cementation control the evolution of porosity in the deep layers. The whole process is continuous, the trend of decreasing porosity in the shallow and deep layers is consistent, and the effect-oriented model of decreasing porosity is successional and consistent (Fig. 4). Therefore, the pore volume reduction of the shallow and deep layers can be obtained from the same model.

Athy (1930) provided a model postulating that the porosity of mudstone is an exponential function of the burial depth in normal compaction conditions. This model has been applied in the study of sandstone for a long time. However, in-depth studies found that the porosity of sandstone is not only related to burial depth but also to geological age (Maxwell, 1964; Schere, 1987; Hayes, 1991; Ehrenberg et al, 2009).

Liu et al (2007b) demonstrated that porosity can be expressed as a binary function of burial time and burial depth; therefore, when the burial depth and the burial time are obtained, the porosity of sandstone can be computed using multiple regression analysis. Therefore, the following decreasing porosity model is established.

$$\phi_n = 48\mathrm{e}^{(-0.00057z+0.0003t+0.00000052zt)} \tag{1}$$

ϕ_n: residual porosity after compacting and cementing, %; z: burial depth, m; t: burial time, Ma.

3.3 Increasing porosity model

Increase in porosity is known to be generated by solution, which is a result of organic acids dissolving minerals such as carbonate and feldspar when the temperature is within a specific range (Carothers and Kharaka, 1978; Surdam et

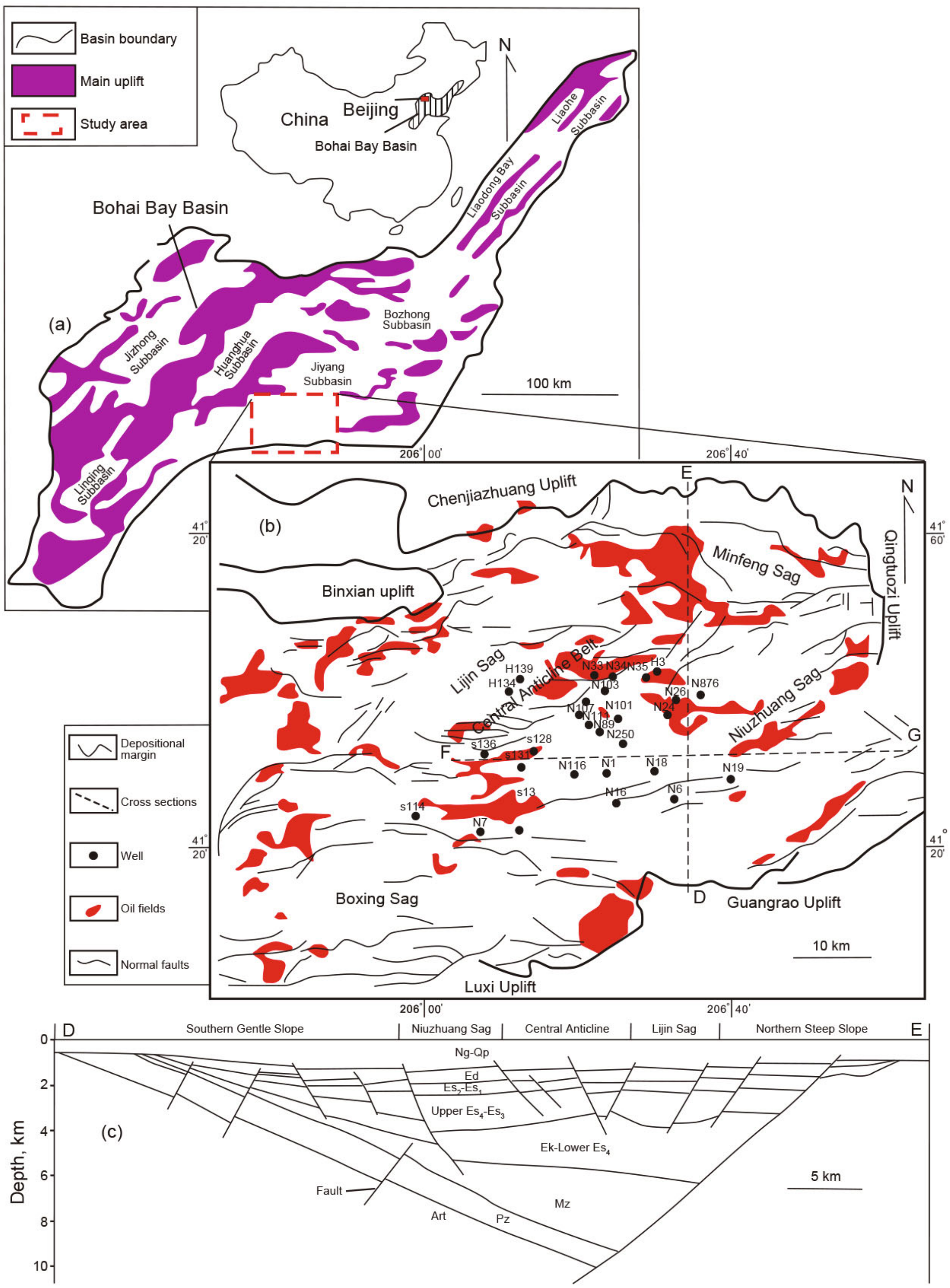

Fig. 1 (a) Location map showing the six major subbasins of the Bohai Bay Basin. (b) Oil field distribution, the locations of sections DE and FG, wells and normal faults for the top of Es_3 interval in the study area. (c) Cross section DE showing the different tectonic-structural zones and key stratigraphic intervals

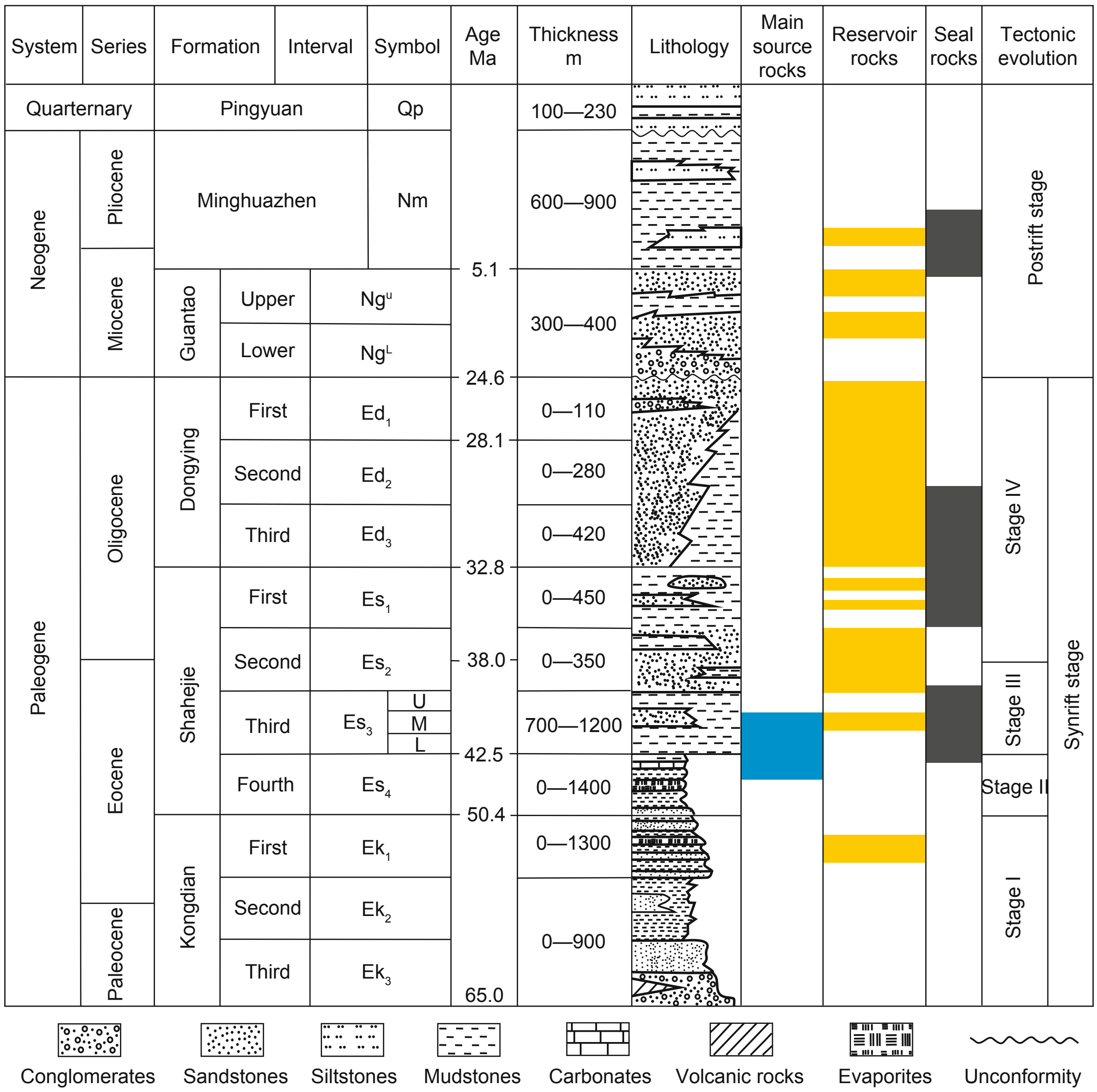

Fig. 2 Schematic Cenozoic-Quaternary stratigraphy of the Niuzhuang Sag, showing tectonic evolution stages and the major petroleum system elements

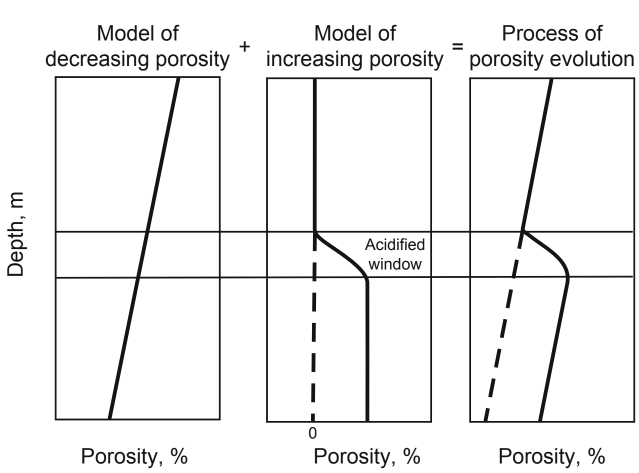

Fig. 3 The model of porosity evolution, which is divided into the decreasing porosity model and the increasing porosity model

al, 1984; 1989; Zhang et al, 2009; Schieber, 2011). With regard to the Niuzhuang Sag, Chen et al (2009) proposed that carbonate cements were dissolved in the Jiyang sub basin when the paleotemperature was about 70 °C. The timing of the oil charge in the Dongying Depression is inferred to be around 24 Ma to 20 Ma (Guo et al, 2012a), during which time the temperature in the Niuzhuang Sag was about 90 °C (Fig. 5). As the hydrocarbon charging inhibits mineral dissolution further (Johnson, 1920; Hawkins, 1978; Hayes, 1991), we define the acidified window as the period when the geothermal temperature ranged from 70 °C to 90 °C. If the temperature was below 70 °C, the organic acid was insufficient to generate secondary porosity. If the temperature was over 90 °C, the solution became weak because of the reduction of the concentration of organic acids and hydrocarbon emplacement.

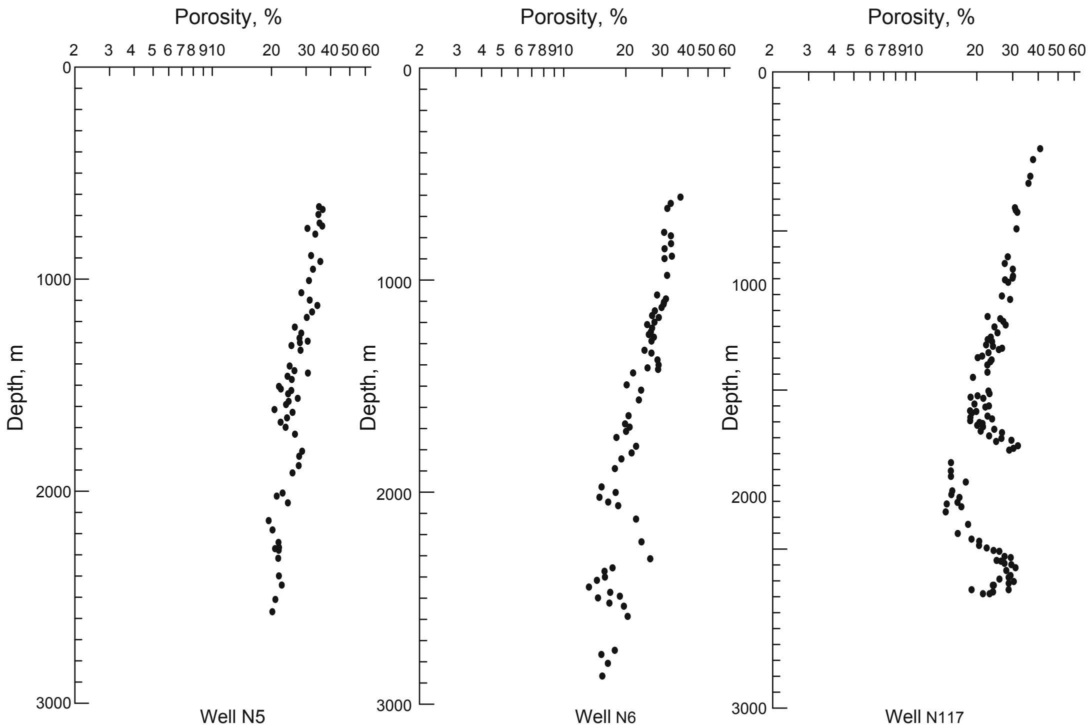

Fig. 4 Porosity sections of typical wells in the Niuzhuang Sag showing that the trend of decreasing porosity is consistent between shallow and deep layers

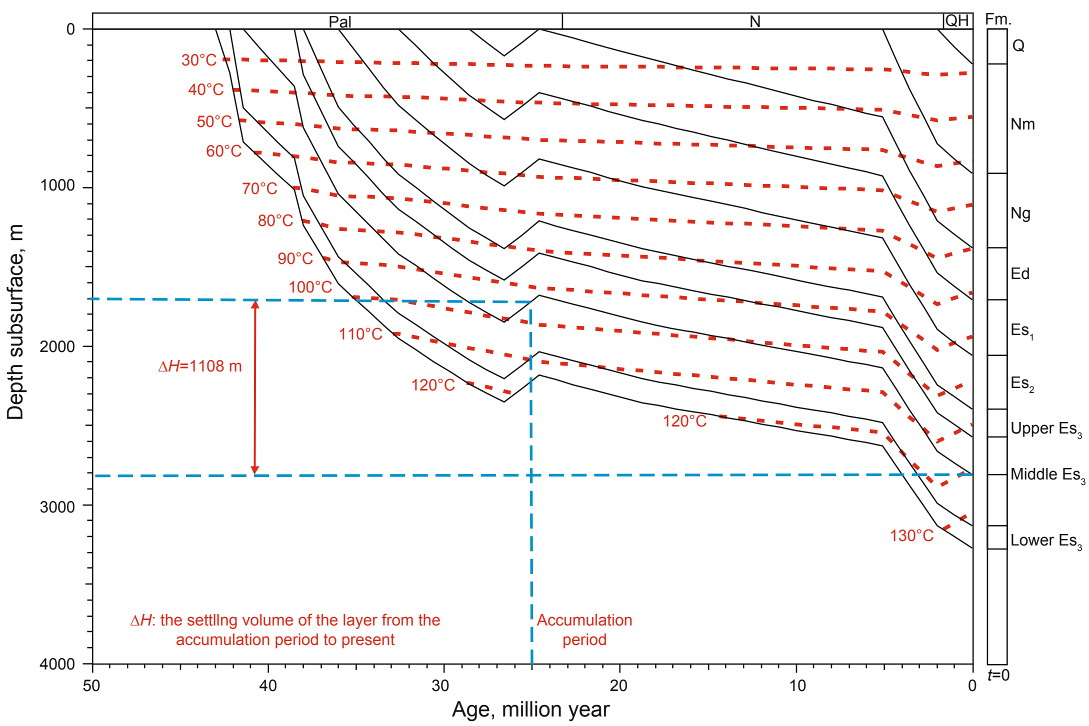

Fig. 5 The burial and thermal history map of well N6 in Niuzhuang Sag, which shows the Middle Es_3 Member subsided about 1108m in the process from the accumulation period to present

According to the theory of chemical dynamics, reaction rate is proportional to concentration. Therefore, the dissolution rate of a mineral is proportional to the acid concentration such that

$$\frac{\partial \phi_s}{\partial t} = k_1^{'}C + c_0^{'} \quad (2)$$

ϕ_s: secondary porosity due to denudation, %; $k_1^{'}$: constant of proportionality; C: concentration of the organic acid, mol/L; $c_0^{'}$: undetermined constant.

When the concentration of the organic acids in the formation water of the Niuzhuang Sag reached the maximum level, the corresponding geothermal temperature was about 80

°C. Therefore, we establish the relationship between organic acid concentration and geothermal temperature as follows:

$$C = a_1T^2 + b_1T + c_1 \tag{3}$$

T: formation temperature, °C; a_1, b_1, c_1: undetermined constants.

In a particular period, burial depth is proportional to burial time and to the geothermal temperature. Therefore, the change rate of porosity in the acidified window can be modeled as follows:

$$\frac{\partial \phi_s}{\partial t} = a't^2 + b't + c' \tag{4}$$

a', b', c': undetermined constants.

We convert the time to geohistorical time, define the time when the geothermal temperature first reaches 70 °C as t_1, and set the time when the geothermal temperature first reaches 90 °C as t_2. When $t=t_1$, $\phi_s=0$; $t=t_2$, $\phi_s=\Delta\phi$. As the curve of increasing porosity is centrosymmetric, we can solve the equation above and obtain the model of the secondary porosity increment in the acidified window.

$$\phi_s = -\frac{2\Delta\phi}{\Delta t^3}(t-t_1)^3 + \frac{3\Delta\phi}{\Delta t^2}(t-t_1)^2 \tag{5}$$

t: burial time, Ma; $\Delta\phi$: actual increment of porosity, %; t_1: time when the geothermal temperature first reaches 70 °C, Ma; t_2: time when the temperature first reaches 90 °C, Ma; Δt: time interval of the layer in the acidified window, Ma; $\Delta t = t_2 - t_1$, Ma.

3.4 The model of paleoporosity estimation

Based on the analysis above, the process of porosity evolution can be divided into three stages: (1) before the layer enters the acidified window, during which no secondary pores are found, and porosity simply decreases by compaction; (2) when the layer is in the acidified window, during which pores are not only increasing by solution but also decreasing by compaction and cementation; and (3) after the layer exits the acidified window, during which the increment of the porosity is constant. At this stage, the layer is compacted based on the secondary pores. We can then estimate the paleoporosity as follows:

$$\phi = \begin{cases} \phi_0 e^{(az+bt+czt)} & t \geq t_1 \\ \phi_0 e^{(az+bt+czt)} - \frac{2\Delta\phi}{\Delta t^3}(t-t_1)^3 + \frac{3\Delta\phi}{\Delta t^2}(t-t_1)^2 & t_1 > t > t_2 \\ \phi_0 e^{(az+bt+czt)} + \Delta\phi & t \leq t_2 \end{cases} \tag{6}$$

ϕ_0: initial porosity, %; Δt: time interval of the layer in the acidified window, Ma; $\Delta t = t_2 - t_1$; a, b, c: constants of the binary function.

Based on the present lower porosity limit of the reservoir and with the aid of burial history research, the current study determines the critical porosity by tracing the porosity section from the present time back to the accumulation period (Pan et al, 2011a; Guo et al, 2012b; Liu et al, 2012). The paleoporosity is estimated using the principle of effect-oriented simulation with the current porosity as the boundary constraint condition (Pan et al, 2011b; Guo et al, 2012b).

Therefore, the rule of hydrocarbon accumulation and enrichment is demonstrated by comparing paleoporosity with the critical porosity and by analyzing the distribution relationship between paleoporosity and the reservoir.

4 Results

4.1 Cutoff value of the present reservoir

In this study, the cutoff value of the present reservoir is determined by the cross-plot method of porosity and permeability and the oil occurrence method (Pan et al, 2011a; Jin et al, 2012; Guo et al, 2012b; Liu et al, 2012) based on well testing and core logging data.

4.1.1 Data statistics of well testing

The relationship between well testing and reservoir properties is established by using relevant data from the middle Es_3 member. In the oil layer, porosity ranges from 3.5% to 25.8%, and permeability ranges from 0.09×10^{-3} μm^2 to 387×10^{-3} μm^2. In the water zone, porosity ranges from 2.2% to 26.1%, and permeability ranges from 0.05×10^{-3} μm^2 to 644×10^{-3} μm^2. In the dry bed, porosity ranges from 3.7% to 23.8%, and permeability ranges from 0.04×10^{-3} μm^2 to 222×10^{-3} μm^2. The data suggest that a complex relationship exists between the reservoir properties and hydrocarbon. A reservoir with good properties may not be an oil layer, but it may be a water zone or even a dry bed. Conversely, a reservoir with poor properties can be an oil layer. The reservoir with properties of equal value can be an oil layer, water zone, or a dry bed. A porosity of 3.5% and a permeability of 0.09×10^{-3} μm^2 are the cutoff values obtained from the well testing data (Fig. 6).

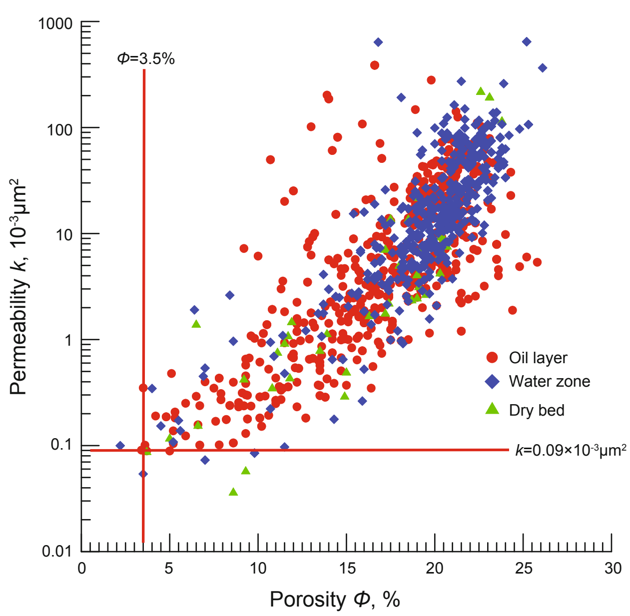

Fig. 6 Cross-plot of porosity versus permeability with well test result, which shows the cutoff values of middle Es_3 member in the Niuzhuang Sag

4.1.2 Data statistics of core logging

Similarly, the relationship between core logging and reservoir properties is established using relevant data from the middle Es_3 member. For the oil-rich sandstone, porosity ranges from 6.5% to 22.4%, and permeability ranges from 0.24 × 10^{-3} μm^2 to 24.2 × 10^{-3} μm^2. For the oil-soaked sandstone, porosity ranges from 3.5% to 24.9%, and permeability ranges from 0.1 × 10^{-3} μm^2 to 387 × 10^{-3} μm^2. For fluorescent sandstone, porosity ranges from 15.3% to 21.3%, and permeability ranges from 2.13 × 10^{-3} μm^2 to 19.3 × 10^{-3} μm^2. The sandstone property that indicates oil occurrence has no strict boundaries. These values suggest an irregular relationship between reservoir properties and hydrocarbon. The sandstones with properties of high value may be fluorescent, whereas those with properties of low value may be oil rich sandstones. A porosity of 3.5% and a permeability of 0.1 × 10^{-3} μm^2 are the cutoff values obtained from the well logging data (Fig. 7).

By comprehensively analyzing the cutoff values obtained from the well testing and core logging data, the cutoff values of the present reservoir in the middle Es_3 member of the Niuzhuang Sag are defined as follows: porosity is 3.5%, and permeability is 0.095 × 10^{-3} μm^2.

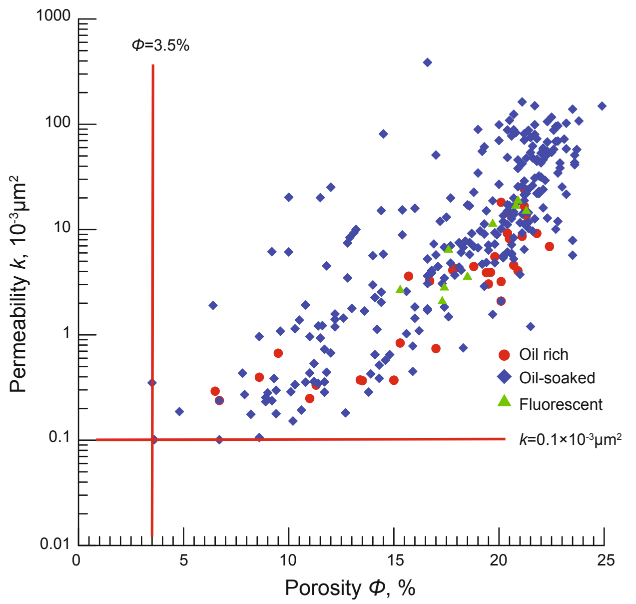

Fig. 7 Cross-plot of porosity versus permeability with well log results, which shows the permeability and porosity cutoff values of the middle Es_3 member in the Niuzhuang Sag

4.2 Critical property in the accumulation period

After the accumulation period, the middle Es_3 member subsided and reached the present maximum burial depth. Thus typical wells can be selected to first obtain the present porosity section. The porosity section in the maximum burial period is estimated subsequently. According to the evolution trend of the porosity section at the maximum burial depth, we trace the difference between the maximum burial depth and the depth during the accumulation period to estimate the porosity section during the accumulation period. The porosity variation is the difference in porosity between the accumulation period and the present after reservoir formation. By adding the porosity variation and the present cutoff value, the critical porosity during the accumulation period can be obtained.

Several studies have investigated the accumulation period in the Dongying Depression or Niuzhuang Sag (Qiu et al, 2000; Jiang et al, 2003; Zhu et al, 2004; Zhu et al, 2007; Guo et al, 2012a). The results of these studies show that the hydrocarbon in the middle Es_3 member accumulated mainly at the time of the end of the Dongying Formation and at the beginning of the Guantao Formation (25 Ma). Both stages are the focus of the current work to estimate paleoporosity.

In the present study, five typical wells were selected to calculate the critical porosity. In the following discussion, N6 is used as an example.

The burial and geothermal histories of well N6 suggest that hydrocarbon accumulated at the end of the uplifting in 25 Ma (Fig. 5). It was then uplifted for a short period and then continuously subsided until the present time, reaching its maximum burial depth. The strata subsided by 1,108 m from the accumulation period to the maximum burial period. Using the present porosity of 12.7% and tracing back about 1,108 m according to the porosity section, we determine that the porosity in the accumulation period is 24.7%. Therefore, the porosity variation from the accumulation period to the maximum burial period is 12% (Fig. 8). By adding the average porosity variation values of the five wells (Table 1) and the present cutoff values of reservoir porosity, the critical porosity of the reservoir is determined to be 13.9%.

4.3 Paleoporosity estimation in the accumulation period

Paleoporosity estimation is a difficult problem, and researchers have proposed various methods from different aspects (Meng et al, 2003; Pan et al, 2011b; Qu et al, 2012). Inspired by the methods of Pan et al (2011b) and Guo et al (2012b), the present study uses the principle of effect-oriented simulation with current porosity as the boundary constraint condition. Therefore, porosity evolution can be divided into two processes: increasing porosity and decreasing porosity. The superimposition of the two effects comprises the porosity evolution process; thus, paleoporosity can be estimated from geological history.

With well N117 as an example, we choose the point with a burial depth of 2,902 m and present porosity of 15.9% to simulate porosity evolution from the aspects of time (Fig. 9(a)), burial depth (Fig. 9(b)) and synthesized evolution (Fig. 9(c)) respectively.

1) The depositing of the middle Es_3 member began in 42.1 Ma, and the primary porosity was 48%.

2) The strata subsided continuously until the burial depth was 1,049 m in 35.7 Ma. Meanwhile, the porosity decreased to 26.5% because of compaction.

3) The strata were in the acidified window from 35.7 Ma to 30.4 Ma, when the geothermal temperature was 70 °C to 90 °C. The organic acid fluid eroded the minerals and formed secondary pores. The secondary porosity was 5.8% when hydrocarbon was charged in 30.4 Ma. The porosity

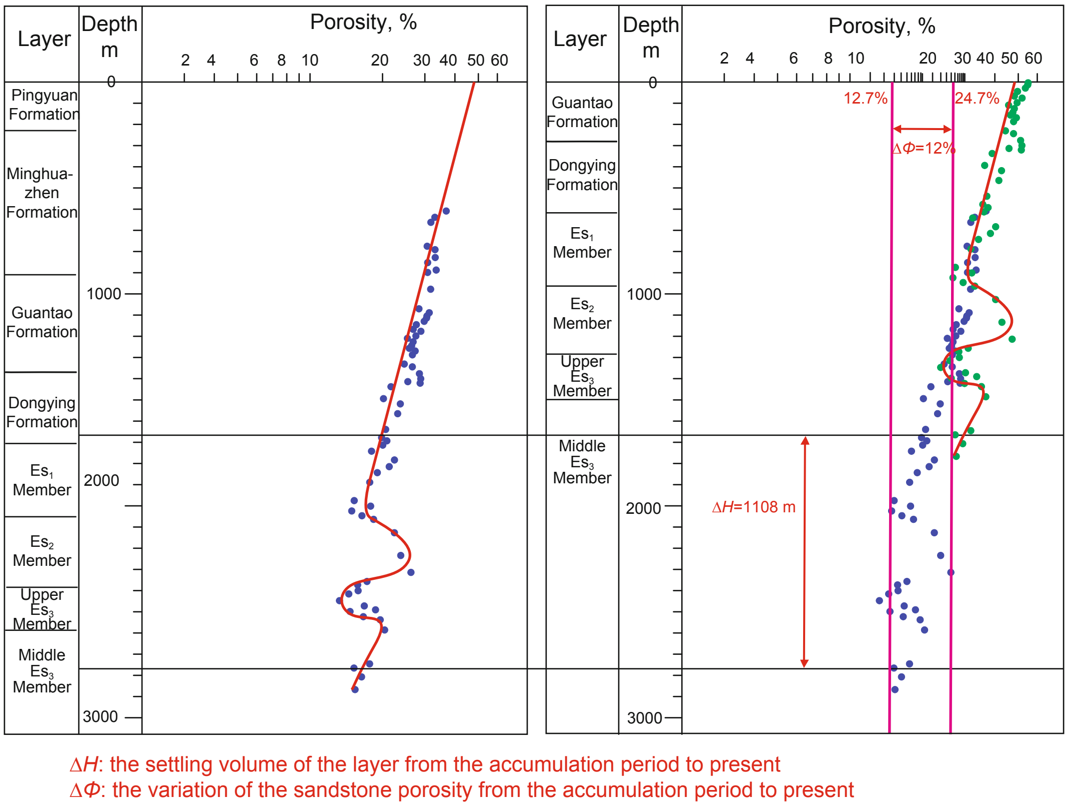

Fig. 8 The porosity section in the maximum burial depth period (left) and the porosity section in the accumulation period (right), which shows the porosity variation between the two stages of middle Es_3 member in the Niuzhuang Sag

Table 1 Porosity variation between accumulation period and the maximum burial period of typical wells in the Niuzhuang Sag

Well name	Decrease in porosity, %	Average value
N117	10.4	
N7	10.1	
N8	9.7	10.4%
N5	10	
N6	12	

decreased by 6.2% as a result of compaction and cementation. Therefore, the porosity actually decreased by 0.4% to 26.1%.

4) The strata subsided continuously from 30.4 Ma to 26.6 Ma until the burial depth was 1,876.9 m. Meanwhile, the porosity decreased to 22.7% because of compaction and cementation.

5) The strata were uplifted from 26.6 Ma to 24.5 Ma, and burial depth was shallower than the previous maximum burial depth. Therefore, burial depth had no effect on porosity. However, porosity still decreased weakly by 0.1% with time.

6) The strata subsided continuously from 24.5 Ma until the present time, reaching the maximum burial depth. The porosity decreased by 6.7% because of compaction and cementation; at present, the porosity is 15.9%.

The middle Es_3 member in the western part of the Niuzhuang Sag shows six stages of delta growth (Fig. 10), which can be recognized by seismic reflection terminal relations as onlap, truncation, and downlap. T4 and T6 are the top and bottom layers of the middle Es_3 member, respectively. T51, T52, T53, T54, and T55 are the division surfaces of the six stages. This study selects 26 wells to estimate the paleoporosity of T53 and 28 wells for T54 (Table 2).

5 Discussion

5.1 The relationship between paleoporosity and critical porosity

Table 2 suggests that the porosity of producing and dry wells is greater than the critical porosity during the accumulation period. This result indicates that the reservoirs of the middle Es_3 member could all have been charged by hydrocarbon.

5.2 The control of paleoporosity on hydrocarbon accumulation

According to the relation of paleoporosity isograms and reservoir distribution (Figs. 11 and 12, respectively), paleoporosity is demonstrated to be high in the east and low in the west. Furthermore, an apparent boundary exists between the reservoir region and the dry area. In the producing wells, paleoporosity ranges from 21.9% to 24.5%; paleoporosity of the dry wells ranges from 18.8% to 23.2%. The reservoir is mainly developed in the area where the paleoporosity is greater than 22% at the top of T53. At the top of T54, the paleoporosity of the producing wells mainly ranges from 21.2% to 23.9%, whereas that of the dry wells ranges from 18.3% to 21.8%. The reservoir is mainly developed in the

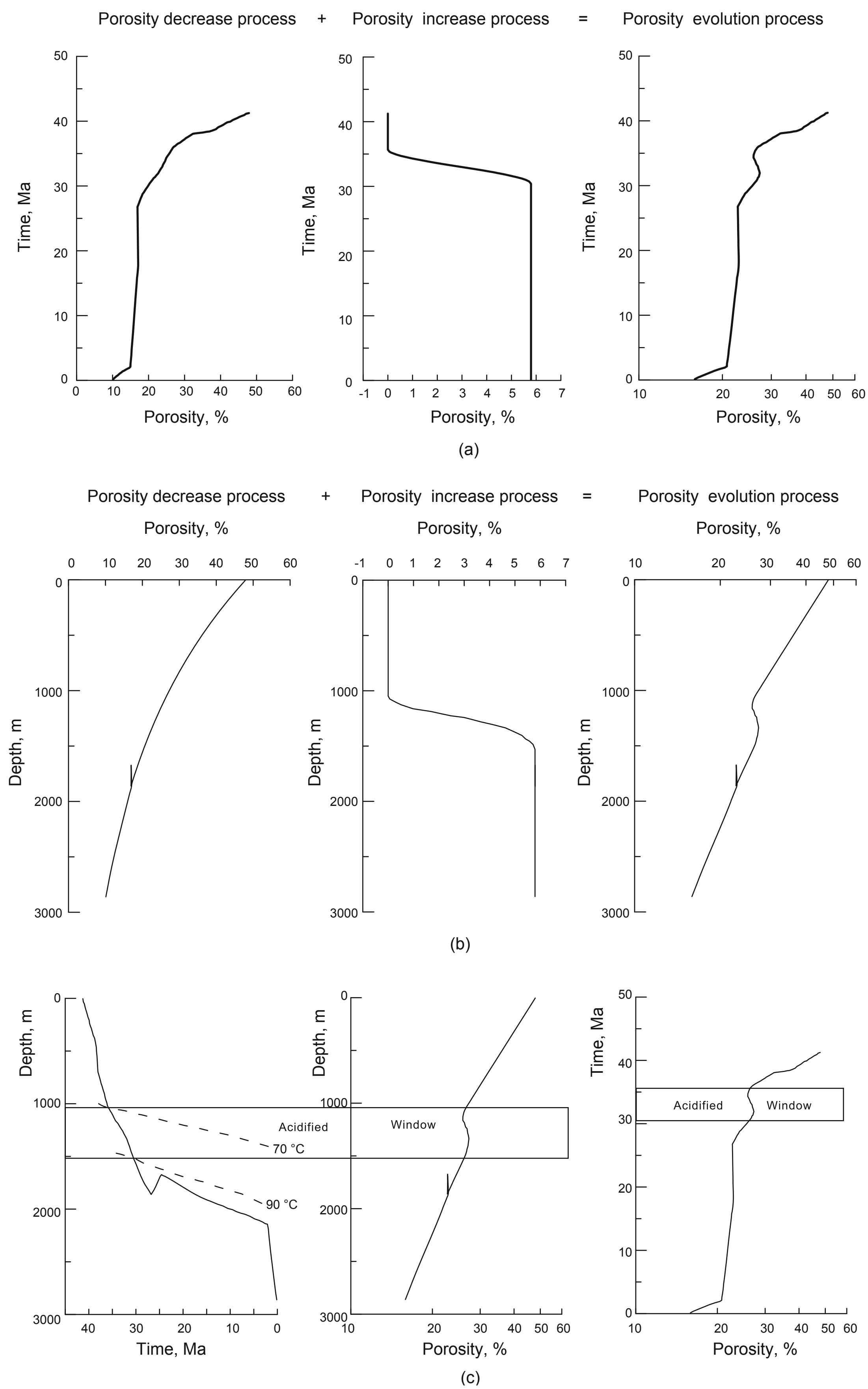

Fig. 9 The simulation of sandstone porosity evolution of well N117 from time (a), depth (b), and synthesized evolution (c) respectively

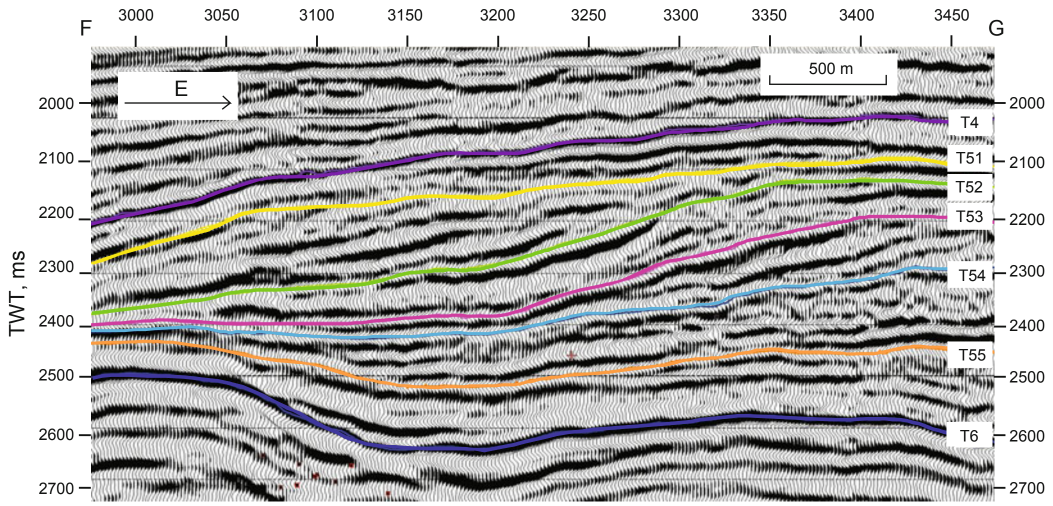

Fig. 10 Division of sandstone set of middle Es_3 member in the Niuzhuang Sag, which consists of six stages of delta deposition

Table 2 Paleoporosity of typical wells in the accumulation period of the Niuzhuang Sag

Well name	Paleoporosity of T53	Paleoporosity of T54	Well name	Paleoporosity of T53	Paleoporosity of T54
N101	24.5%	23.6%	S136	\	21.2%
N106	22.8%	22.0%	S114	20.4%	18.4%
N107	21.7%	21.2%	N19	24.1%	23.9%
N111	21.7%	21.0%	N24	23.01%	21.2%
N16	22.2%	21.8%	S13	20.0%	19.1%
N26	21.8%	21.1%	H3	23.7%	22.8%
N33	22.3%	21.5%	N103	22.7%	22.6%
N34	21.9%	21.6%	S128	24.1%	21.2%
N6	23.7%	22.7%	S131	\	23.3%
N89	21.6%	20.9%	N1	23.6%	21.9%
N18	23.2%	21.8%	N35	22.4%	21.6%
N7	20.3%	19.3%	N116	20.2%	19.8%
H139	19.6%	19.5%	N876	23.8%	22.4%
H134	18.8%	18.3%	N250	22.4%	21.5%

area where the paleoporosity is greater than 20.6%. This result suggests that hydrocarbon enrichment is affected by paleoporosity to some extent.

5.3 The relationship between dominant migration pathways and hydrocarbon accumulation

The dominant migration pathway is defined as a passageway that hydrocarbon goes through in the secondary migration, during which no outside interference emerges. The interaction of several factors forms this pathway: the anisotropy of the system, the heterogeneity of the energy field, and the flow of fluid (Dembicki and Anderson, 1989; Hindle, 1997; Chen et al, 2007; Luo et al, 2007; Pang et al, 2008; Lei et al, 2013). The dominant migration pathways may be faults, unconformable surfaces, or beds with high porosity and permeability. Traps in the dominant migration pathways are prone to hydrocarbon accumulation.

By analyzing the relation of paleoporosity and hydrocarbon formation and enrichment, the study concludes that the reservoirs of the middle Es_3 member mainly have differential dominant pathways, which were formed as a result of the difference in porosity and permeability distribution of the target strata. The delta prograded into the basin from east to west during the deposition of the Dongying Formation; therefore, paleoporosity is high in the east and low in the west. Hydrocarbon always migrates along the dominant migration pathways with superior properties and accumulates in sandstones with high porosity. This result indicates that hydrocarbon accumulation is controlled by the properties of the reservoir in the accumulation period (Fig. 13).

6 Conclusions

1) The paleoporosity of the middle Es_3 member is estimated with the principle of effect-oriented simulation and with the use of current porosity as the boundary constraint condition in the accumulation period, which covers time of the end of the Dongying Formation and the beginning of the Guantao Formation. The critical porosity of the middle Es_3 member in the Niuzhuang Sag is determined to be 13.9% based on the cutoff value of present reservoirs.

2) In comparing the relationship between critical porosity and paleoporosity in the accumulation period of 16 producing wells and 11 dry wells, the paleoporosity of both types of wells is found to be greater than the critical porosity. Therefore, all wells could have been charged by hydrocarbon in the accumulation period. The difference in porosity variation after accumulation leads to the inconsistency between present properties and oiliness.

3) The conformity between contour and reservoir distribution at the top of T53 and T54 indicates the existence of a significant boundary between the reservoir area and the dry region. The hydrocarbon mainly accumulates in reservoirs with high paleoporosity so the paleoporosity of sandstone in the accumulation period affects the distribution

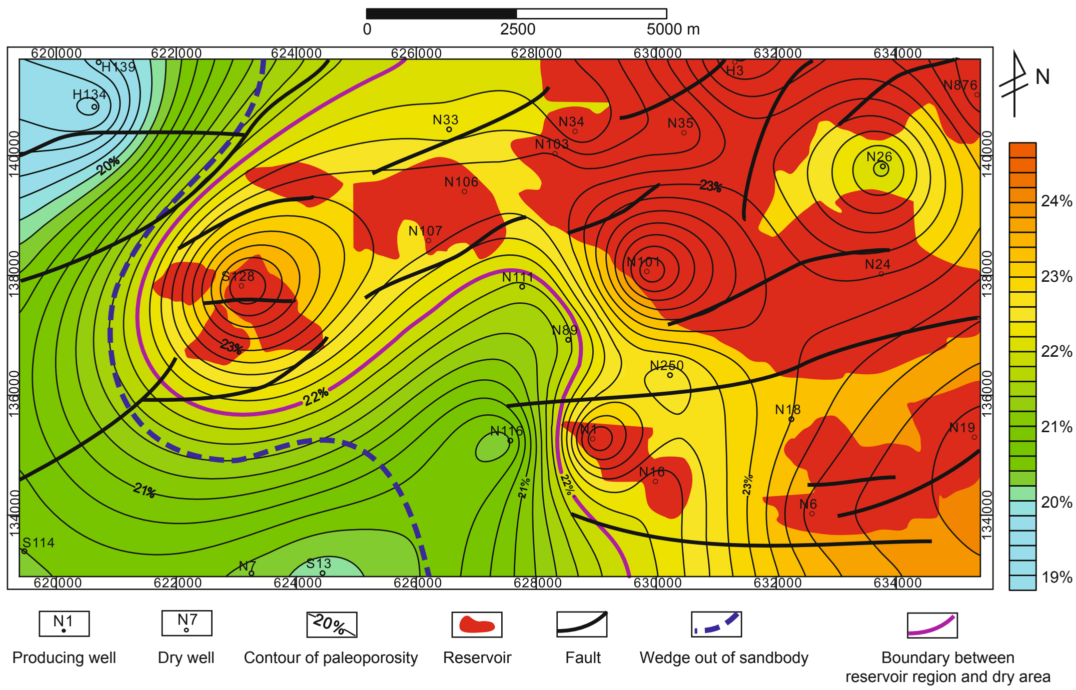

Fig. 11 The relationship between the paleoporosity and reservoir distribution on the top of T53 in the accumulation period of the Niuzhuang Sag

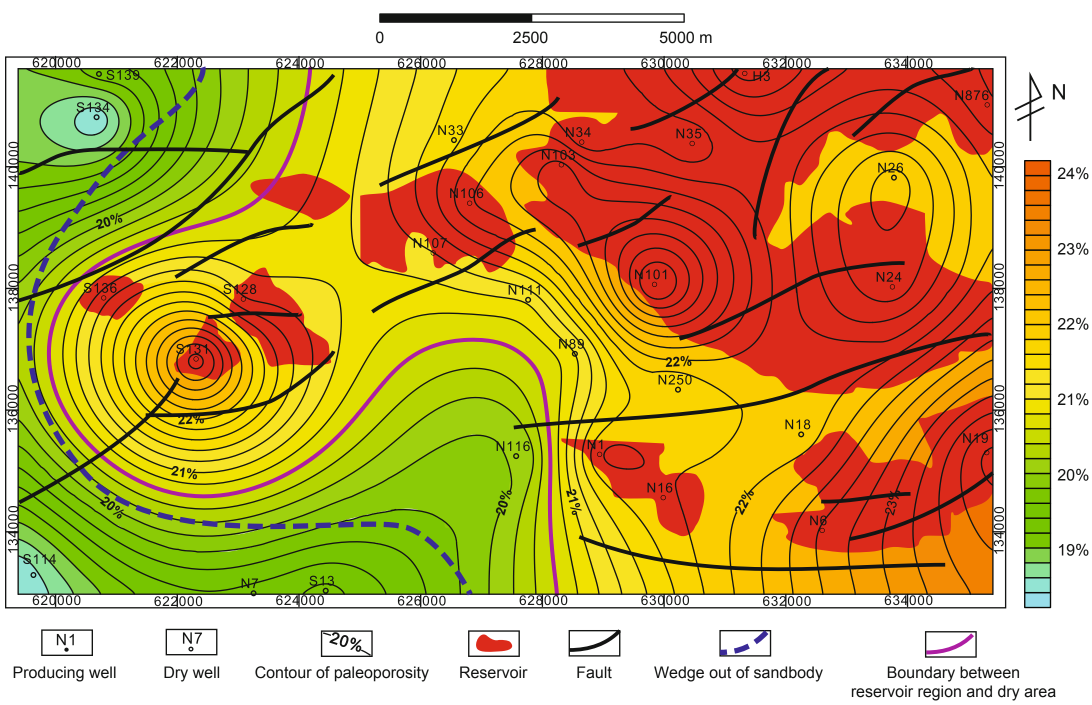

Fig. 12 The relationship between the paleoporosity and reservoir distribution on the top of T54 in the accumulation period of the Niuzhuang Sag

of hydrocarbon.

4) The sandstone reservoirs of the middle Es_3 member in the Niuzhuang Sag with similar fault conduction systems as well as inconsistent present porosity and oiliness generate the dominant migration pathways as a result of the differences in reservoir paleoporosity. Oil and gas tend to be trapped in the dominant migration pathways; therefore, hydrocarbon accumulation and enrichment are controlled by the reservoir paleoporosity.

Acknowledgements

This study is supported by the Young Scholars Development Fund of SWPU. The Xianhe Production Factory of SINOPEC Shengli Oilfield Company is gratefully acknowledged for providing the data used in this study. The reviewers as well as Liu Shifei, Meng Hao, Liang Xinping and Lei Qiao are thanked for their constructive review that helped improve the manuscript.

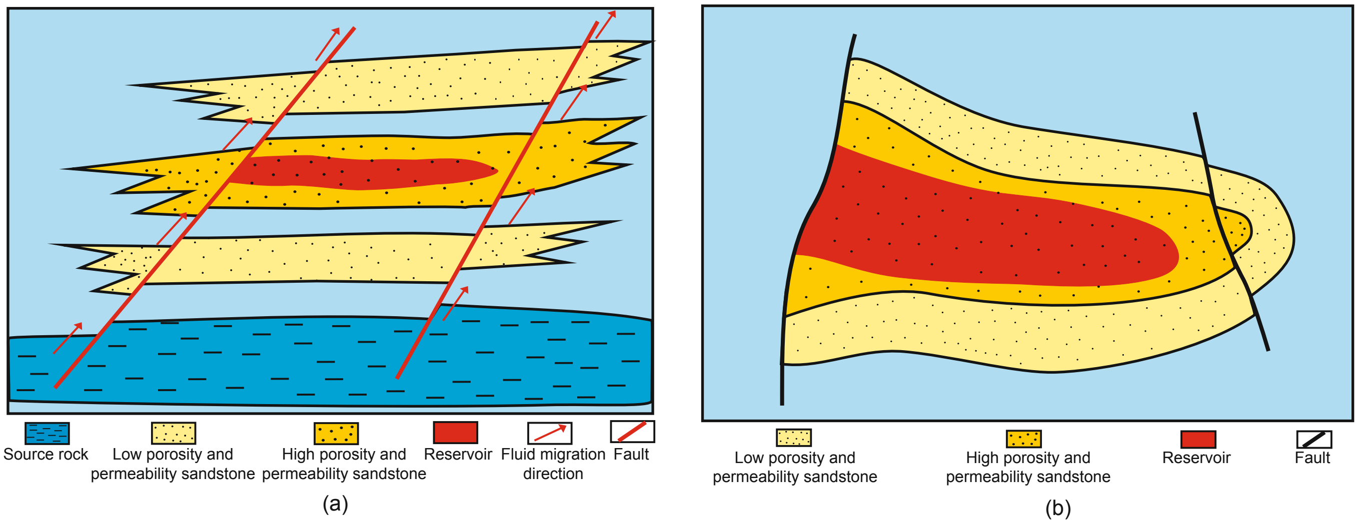

Fig. 13 The section model (a) and the plan model (b) of the hydrocarbon dominant migration pathways generated by paleoporosity differences which control the hydrocarbon accumulation in the Niuzhuang Sag

References

Athy L F. Density, porosity and compaction of sedimentary rock. AAPG Bulletin. 1930. 14(1): 1-24

Cao Y C, Wang Y Z, Xu T Y, et al. The petrophysical parameter cutoff and controlling factors of the effective reservoir of beach and bar sandbodies of the upper part of the fourth menber of the Shahejie formation in west part of Dongying Depression. Acta Sedimentologica Sinica. 2009. 32(2): 230-237 (in Chinese)

Carothers W W and Kharaka Y K. Aliphatic acid anions in oil-field waters: Implications for origin of natural gas. AAPG Bulletin. 1978. 62(12): 2441-2453

Chen D X, Pang X Q, Jiang Z X, et al. Reservoir characteristics and their effects on hydrocarbon accumulation in lacustrine turbidites in the Jiangyang Super-depression, Bohai Bay Basin, China. Marine and Petroleum Geology. 2009. 26(5): 149-162

Chen D X, Pang X Q, Zhang J, et al. Application of quantitative grain fluorescence techniques to study subtle oil migration pathway of lithological reservoir. Frontiers of Earth Science. 2007. 1(4): 498-504

Chen D X, Pang X Q, Zhang S W, et al. Control of facies/potential on hydrocarbon accumulation: a geological model for lacustrine rift basins. Petroleum Science. 2008. 5(3): 212-222

Chen K, Liu Z, Pan G F, et al. Dynamic analysis of lithologic-trap reservoirs in oil-bearing basins—an example from the Chang-8 reservoir in Xifeng area, Ordos Basin. Xinjiang Petroleum Geology. 2012. 33(4): 424-427 (in Chinese)

Dembicki H J and Anderson M J. Secondary migration of oil: Experiments supporting efficient movement of separate, buoyant oil phase along limited conduits. AAPG Bulletin. 1989. 84(1): 65-74

Ehrenberg S N, Nadeau P H and Steen Φ. Petroleum reservoir porosity versus depth: Influence of geological age. AAPG Bulletin. 2009. 93(10): 1281-1296

Gong Z S. Giant Offshore Oil and Gas Fields in China. Beijing: Petroleum Industry Press. 1997. 396-397 (in Chinese)

Guo R. Supplement to determining method of cut-off value of net play. Petroleum Exploration and Development. 2004. 31(5): 140-144 (in Chinese)

Guo X W, He S, Liu K Y, et al. Oil generation as the dominant overpressure mechanism in the Cenozoic Dongying Depression, Bohai Bay Basin, China. AAPG Bulletin. 2010. 94(12): 1859-1881

Guo X W, Liu K Y, He S, et al. Petroleum generation and charge history of the northern Dongying Depression, Bohai Bay Basin, China: Insight from integrated fluid inclusion analysis and basin modelling. Marine and Petroleum Geology. 2012a. 32(1): 21-35

Guo Y R, Liu J B, Yang H, et al. Hydrocarbon accumulation mechanism of low permeable tight lithologic oil reservoirs in the Yanchang Formation, Ordos Basin, China. Petroleum Exploration and Development. 2012b. 39(4): 417-425 (in Chinese)

Hawkins P J. Relationship between diagenesis, porosity reduction, and oil emplacement in late Carboniferous sandstone reservoirs, Bothamsall Oilfield, E Midlands. Journal of the Geological Society. 1978. 135: 7-24

Hayes J B. Porosity evolution of sandstone relates to vitrinite reflectance. Organic Geochemistry. 1991. 17(2): 117-129

Hindle A D. Petroleum migration pathways and charge concentration: A three-dimensional model. AAPG Bulletin. 1997. 81(9): 1451-1481

Hu S B, O'Sullivan P B, Raza A, et al. Thermal history and tectonic subsidence of the Bohai Basin, northern China: A Cenozoic rifted and local pullapart basin. Physics of the Earth and Planetary Interiors. 2001. 126(3-4): 221-235

Jiang Y L, Liu H, Zhang L, et al. Analysis of petroleum accumulation phase in Dongying Sag. Oil & Gas Geology. 2003. 24(3): 215-218 (in Chinese)

Jiao C H, Xia D D, Wang J, et al. Methods for determining the petrophysical property cutoffs of extra-low porosity and permeability sandstone reservoirs. Oil & Gas Geology. 2009. 30(3): 379-383 (in Chinese)

Jin B, Han J, Jiang S Y, et al. Control of critical physical properties of reservoir to the hydrocarbon accumulation in lithological traps: taking Jurassic of Baijiahai uplift in the eastern Junggar Basin as an example. Journal of Xi'an Shiyou University (Natural Science Edition). 2012. 27(3): 1-7 (in Chinese)

Johnson R H. The cementation process in sandstones. AAPG Bulletin. 1920. 4(1): 33-35

Lampe C, Song G Q, Cong L Z, et al. Fault control on hydrocarbon migration and accumulation in the Tertiary Dongying Depression, Bohai Basin, China. AAPG Bulletin. 2012. 96(6): 983-1000

Lei Y H, Luo X R, Zhang L K, et al. A quantitative method for characterizing transport capability of compound hydrocarbon carrier system. Journal of Earth Science. 2013. 24(3): 328-342

Li L, Zhong D L, Yang C C, et al. The coupling relationship between the west Shandong rise and the Jiyang Depression, China. Journal of Earth Science. 2013. 24(4): 626-644

Li P L. Oil/gas distribution patterns in Dongying Depression, Bohai Bay Basin. Journal of Petroleum Science and Engineering. 2004. 41(1-3): 57-66

Li X S, Zhao Y X, Liu B H, et al. Structural deformation and fault activity of the Tan-Lu fault zone in the Bohai Sea since the late Pleistocene. Chinese Science Bulletin. 2010. 55(18): 1908-1916

Liu Z, Huang Y H, Pan G F, et al. Determination of critical properties of low porosity and permeability sandstone reservoirs and its significance in petroleum geology. Acta Geologica Sinica. 2012. 41(4): 1815-1825 (in Chinese)

Liu Z, Shao X J, Jin B, et al. Co-effect of depth and burial time on the evolution of porosity for clastic rocks during the stage of compaction. Geoscience. 2007b. 21(1): 125-132 (in Chinese)

Liu Z, Zhao Y, Du J H, et al. Characteristics of "multi-factor controlling and key factor entrapping" of formation and distrbution of lithologic petroleum reservoirs in continental rift basin. Chinese Journal of Geology. 2006. 41(4): 612-635 (in Chinese)

Liu Z, Zhao Y, Liang Q S, et al. Formation and Enrichment of Subtle Reservoirs. Beijing: Geological Press. 2007a. 161-162 (in Chinese)

Luo X R, Yu J, Zhang F Q, et al. Numerical modeling of secondary migration and its application to Chang-6 Member of Yanchang Formation (Upper Triassic), Longdong area, Ordos Basin. Science in China Series D: Earth Sciences. 2007. 50(2 Supplement): 91-102

Maxwell J C. Influence of depth, temperature, and geologic age on porosity of quartzose sandstone. AAPG Bulletin. 1964. 48(5): 697-709

Meng Y L, Wang Z G, Yang J S, et al. Comprehensive process-oriented simulation of diagenesis and its application. Petroleum Geology & Experiment. 2003. 25(2): 211-215 (in Chinese)

Pan G F, Liu Z, Zhao S, et al. The study on lower limit of porosity for oil accumulation in Chang-8 Member, Zhenjing area, Ordos Basin. Geoscience. 2011a. 25(2): 271-278 (in Chinese)

Pan G F, Liu Z, Zhao S, et al. Quantitative simulation of sandstone porosity evolution: a case from Yanchang Formation of Zhenjing area, Ordos Basin. Acta Petrolei Sinica. 2011b. 32(2): 249-256 (in Chinese)

Pang X Q, Chen D X, Li P L, et al. Accumulation thresholds of sand lens and controlling mechanism for oil and gas distribution. Acta Petrolei Sinica. 2003. 24(3): 38-45 (in Chinese)

Pang X Q, Chen D X, Zhang S W, et al. Hydrocarbon accumulation in network and its application in the continental rift basin. Science in China Series D: Earth Sciences. 2008. 51(2 Supplement): 88-100

Qi J F, Zhou X H, Deng R J, et al. Structural characteristics of the Tan-Lu fault zone in Cenozoic basins offshore the Bohai Sea. Science in China Series D: Earth Sciences. 2008. 51(2 Supplement): 20-31

Qiu N S, Jin Z J and Hu W X. Study on the hydrocarbon charge history in Dongying Depression: by evidence from fluid inclusions. Journal of China University of Petroleum (Edition of Natural Science). 2000. 24(4): 95-97 (in Chinese)

Qu D F, Jiang Z X, Liu H M, et al. A reconstruction method of porosity for clastic reservoirs during the crucial period of hydrocarbon accumulation. Acta Petrolei Sinica. 2012. 33(3): 404-413 (in Chinese)

Schere M. Parameters influencing porosity in sandstones: A model for sandstone porosity prediction. AAPG Bulletin. 1987. 71(5): 485-491

Schieber J. Marcasite black shale—a mineral proxy for oxygenated bottom waters and intermittent oxidation of carbonaceous muds. Journal of Sedimentary Research. 2011. 81: 447-458

Surdam R C, Boese S W and Crossey L J. The chemistry of secondary porosity. AAPG Memoir. 1984. 37: 127-149

Surdam R C, Crossey L J, Hangen E S, et al. Organic-inorganic interactions and sandstone diagenesis. AAPG Bulletin. 1989. 73(1): 1-23

Wang Y Z, Cao Y C, Song G Q, et al. Determination of physical property lower limit of deep clastic effective reservoirs of Paleogene in Dongying Depression. Journal of China University of Petroleum (Edition of Natural Science). 2009. 33(4): 16-21 (in Chinese)

Zhang J L, Li D Y and Jiang Z Q. Diagenesis and reservoir quality of the fourth member sandstones of Shahejie Formation in Huimin Depression, eastern China. Journal of Central South University of Technology. 2010. 17(1): 169-179

Zhang L Y, Liu Q, Zhu R F, et al. Source rocks in Mesozoic-Cenozoic continental rift basins, east China: a case from the Dongying Depression, Bohai Bay Basin. Organic Geochemistry. 2009. 40(2): 229-242

Zhang S W, Wang Y S, Shi D S, et al. Fault-fracture mesh petroleum plays in the Jiyang Superdepression of the Bohai Bay Basin, eastern China. Marine and Petroleum Geology. 2004. 21(6): 651-668

Zhang Y W, Zeng J H and Yu B S. Experimental study on interaction between simulated sandstone and acidic fluid. Petroleum Science. 2009. 6(1): 8-16

Zhu G Y, Jin Q, Dai J X, et al. A study on periods of hydrocarbon accumulation and distribution pattern of oil and gas pools in Dongying Depression. Oil & Gas Geology. 2004. 25(2): 209-215 (in Chinese)

Zhu H Q, Pang X Q, Jiang Z X, et al. Accumulation time and accumulation process of lithological reservoirs in Dongying Depression. Geological Science and Technology Information. 2007. 26(1): 65-69 (in Chinese)

Zhu H Q, Pang X Q, Lin S G, et al. The controls on the lithologic oil pools and models for hydrocarbon accumulation in the Dongying Depression, Shandong. Sedimentary Geology and Tethyan Geology. 2006. 26(1): 74-80 (in Chinese)

Zhu J J. Geologic genesis of high oil saturation in low porosity and low permeability reservoirs by taking the reservoir in Dongying Depression in Shengli oil region for example. Journal of Oil and Gas Technology. 2008. 30(3): 64-67 (in Chinese)

(Edited by Hao Jie)